Eur Radiol (2012) 22:1972–1982
DOI 10.1007/s00330-012-2438-x

INTERVENTIONAL

MR-guided radiofrequency ablation using a wide-bore 1.5-T MR system: clinical results of 213 treated liver lesions

Hansjörg Rempp · Lorenz Waibel · Rüdiger Hoffmann · Claus D. Claussen · Philippe L. Pereira · Stephan Clasen

Received: 16 November 2011 / Revised: 26 January 2012 / Accepted: 13 February 2012 / Published online: 18 April 2012

Abstract
Objective To evaluate the technical effectiveness, technical success and patient safety of MR-guided radiofrequency (RF) ablation of liver malignancies using a wide-bore 1.5-T MR system.
Methods In 110 patients, 56 primary liver lesions and 157 liver metastases were treated in 157 sessions using percutaneous RF ablation. Mean lesion diameter was 20 mm (range 4–54 mm). All planning, procedural and post-interventional control MR investigations were carried out using a wide-bore 1.5-T MR system. Technical success was assessed by a contrast-enhanced MR liver examination immediately after the intervention. Technique effectiveness was assessed by dynamic hepatic MR study 1 month post ablation; mean follow-up period was 24.2 months (range 5–44).
Results Technical success and technique effectiveness were achieved in 210/213 lesions (98.6 %). In 18/210 lesions (8.6 %), local tumour progression occurred 4–28 months after therapy. Seven of these 18 lesions were treated in a second session achieving complete ablation, 6 other lesions were referred to surgery. Overall RF effectiveness rate was 199/213 (93.4 %); overall therapy success (including surgery) was 205/213 (96.2 %). Two major complications (1.3 %) (bleeding and infected biloma) and 14 (8.9 %) minor complications occurred subsequent to 157 interventions.
Conclusion Wide-bore MR-guided RF ablation is a safe and effective treatment option for liver lesions.
Key Points
- *Magnetic resonance-guided radiofrequency ablation offers various options for monitoring therapy.*
- *All steps of RF ablation carried out in 1.5-T wide-bore system.*
- *Therapeutic decisions were based on T1-weighted imaging.*
- *Technical success and technical effectiveness were high.*
- *Local tumour progression rate was 8.6 % over a 24-month mean follow-up.*

Keywords Radiofrequency ablation · RFA · Hepatocellular carcinoma · MR-guided intervention · Magnetic resonance imaging

Introduction

Radiofrequency (RF) ablation has become a standard clinical approach to treat focal liver lesions during the last decade [1–4]. The intervention aims to completely ablate the target lesion and, in this respect, has to compete with surgery as a treatment option. The percutaneous approach creates small wounds, only necessitates a short period of hospitalisation and is reasonably cheap [5]. Additionally, only a small amount of healthy liver tissue must be sacrificed. For these reasons, RF ablation has become a recommended therapy for early stage hepatocellular carcinomas [6–8]. For liver metastases, surgical treatment still remains the gold standard therapy and has been proven to improve patients' prognoses. However, resection is not always possible due to the number or location of the metastases [9–11]. A wider indication for RF ablation in the case of secondary liver lesions is currently being discussed

H. Rempp (✉) · L. Waibel · R. Hoffmann · C. D. Claussen · S. Clasen
Department of Diagnostic and Interventional Radiology,
Eberhard Karls University of Tübingen,
Hoppe-Seyler-Straße 3,
72076 Tübingen, Germany
e-mail: hansjoerg.rempp@med.uni-tuebingen.de

P. L. Pereira
Clinic for Radiology, Nuclear Medicine and Minimal Invasive Therapies, SLK-Clinics,
Am Gesundbrunnen 20–26,
74078 Heilbronn, Germany

[12]. One major drawback of RF ablation is that the local tumour progression rate is still high, as reported in several studies [1, 13–15]. Precise therapy monitoring and individual treatment decisions which are based on reliable tumour imaging during the treatment may help to improve therapy outcome. Ultrasound is inexpensive, fast and easily available, although its capacity to visualise treated tissue is restricted [16]. CT offers precise imaging, but the differentiation between vital tumour tissue and the ablation zone is only possible for a limited time after application of a contrast agent [17]. MR guidance has been proposed for RF ablation owing to its high soft-tissue contrast and its capacity to differentiate vital tumour areas from the ablation zone [18, 19]. Wide-bore 1.5-T MR systems can be used for planning, applicator placement, therapy monitoring and controlling. The purpose of this study was to evaluate the technical success, patient safety and long-term effectiveness of MR-guided RF ablation in a mixed group of patients.

Materials and methods

Patients and lesions treated

The institutional review board approved the MR-guided ablation of the patients. The individual therapy decision was made by an interdisciplinary tumour board. All patients signed informed consent to this procedure at least 1 day before treatment. Inclusion criteria were liver metastases with a maximum diameter of 5 cm and hepatocellular carcinomas with a maximum diameter of 6 cm. Exclusion criteria were contraindications to MR imaging and inadequate coagulation status (platelet count below 50,000/μL, Quick test less than 50 %). Patients who had undergone treatment at the same lesion with transcatheter arterial (chemo-)embolisation before RF ablation were excluded from this evaluation. Between 2006 and 2010, 110 patients were included in the study, among them 27 women and 83 men. Mean patient age was 64±10 (mean ± standard deviation); the youngest patient was 29 years old, the eldest was 92 years old. A total of 213 lesions were treated in 157 interventions; 56 lesions were primary liver tumours, comprising 43 hepatocellular carcinomas and 13 cholangiocellular carcinomas; 157 lesions were secondary liver lesions, of which 114 colorectal liver lesions formed the largest group. Other primary tumours were melanomas (21 lesions), breast cancer (9), neuroendocrine carcinomas (7), renal cell carcinomas (2), and cancers of the lung (2) and of the oesophagus (2). The mean lesion size was 20±10 mm; the smallest lesion had a diameter of 4 mm, the largest a diameter of 54 mm. The mean lesion size of the hepatocellular carcinomas was 25.0±9 mm, and 17.7±10 mm for all other lesions.

Patient treatment

All patients were treated using a wide-bore 1.5-T system (Siemens Magnetom Espree, Siemens Healthcare, Erlangen, Germany). Treatment included an MR planning examination, applicator placement using fluoroscopic sequences, repeated control imaging during the ablation procedure and contrast-enhanced post-interventional control imaging.

The patients were positioned supine with feet forward in the wide-bore MR system. A six-channel body array and an additional one-channel loop array placed around the puncture site were used. A planning examination aimed to confirm the number, location and size of the liver lesions and to determine the puncture site and the applicator track. An orientation grid helped to define the puncture site on the skin (TargoGrid™, Invivo Germany GmbH, Schwerin, Germany). The planning examination comprised T1- and T2-weighted sequences and diffusion-weighted imaging (Table 1, Fig. 1). In 16 patients the lesions could not be identified on non-enhanced sequences and a pre-procedural contrast-enhanced dynamic liver examination was performed. Sagittal and coronal angulated T1-weighted slices over the region of interest were acquired as baseline images for further intra-procedural and post-interventional comparison.

The selected puncture site was labelled with a skin marker before skin disinfection. Local anaesthetics were injected subcutaneously (Xylocaine 0.9 %, AstraZeneca, Wedel, Germany) before a small skin incision was made. Analgesia and sedation were applied intravenously (i.v.) during the intervention (analgesia: piritramide i.v., total dose 8–15 mg or pethidine i.v., total dose 50–150 mg; sedation: midazolam i.v., total dose 3–5 mg); pulse rate and oxygen saturation were monitored. Different commercially available MR-compatible RF systems were used [20]. Twenty-six lesions were treated using an internally water-cooled monopolar RF system with 17-gauge single applicators (Valleylab, Covidien, Boulder, CO, USA). The active tip length varied between 3 and 4 cm. Two grounding pads were placed under the patients' backs. Nineteen lesions were treated using a 17-gauge internally water-cooled monopolar cluster applicator with three electrodes located on the same handhold (Valleylab, Covidien, USA). The active tip length was 2.5 cm. Four grounding pads were placed beneath the thigh and back of the patients. A total of 168 lesions were treated using internally water-cooled bi- or multipolar applicators (Olympus Celon, Teltow, Germany). In 21 cases, a single applicator was used in bipolar mode. Two applicators were used in 129 cases, three in 16 cases and four applicators were used in 2 cases. Depending on the tumour diameter, active tip lengths of 2, 3 and 4 cm were used. The RF generator and the fluid pump were placed outside the MR suite and connected to the applicators via a cable tunnel. A magnetically shielded liquid crystal monitor placed beside the interventionalist displayed the acquired images within the MR

Table 1 Sequence details

Sequence	TE (ms)	TR (ms)	Slice thickness (mm)	Matrix	Flip angle (°)	Bandwidth (Hz/pixel)
Planning						
HASTE (coronal)	116	1,100	6	205×256	120	490
T1 in- and opposed phase	2.7	100	6	154×256	70	280
T1 Flash2D	4.14	212	6	256×256	70	140
T2 TSE	101	4,185	6	320×80	150	260
Diffusion (EPI)	82	660	6	128×128	90	1,776
T1 VIBE (optional)	1.58	4.13	2.2	146×256	10	400
Fluoroscopic imaging (targeting)						
BEAT_IRTT (SSFP) predominantly T2W	1.8	829	12	128×128	15	1,028
BEAT_IRTT (SSFP) predominantly T1W	1.97	3.94	12	128×128	70	560
Therapy monitoring						
T1 Flash2D	4.36	122	6	176×256	70	140
T2 TSE	126	3,800	6	320×80	145	260
T2 TrueFISP	2.2	4.4	6	256×256	75	500
Temperature-sensitive measurements (EPI)	8	800	2	128×128	25	400
Follow-up dynamic liver examinations (1.5 T[a])						
T2 HASTE (coronal)	118	1,100	6	205×256	120	488
T1 Flash2D	5.53	100	6	154×256	70	416
T2 TSE	101	4,185	6	320×80	150	250
Diffusion (EPI)	71	6,421	6	144×92	90	1,736
T1 VIBE	1.05	2.95	2.3	146×256	10	558

HASTE half acquisition single shot turbo spin echo sequence, *Flash* fast low angle shot gradient echo sequence, *TSE* turbo spin echo sequence, *BEAT_IRTT (SSFP)* steady-state free precession sequence (Siemens Corporate Research), *TrueFISP* steady-state precession sequence, *EPI* echoplanar imaging sequence (*b* values 0, 400, 800 mm/s^2), *VIBE* volumetric interpolated breath-hold examination

[a] Follow-up imaging was performed on a 1.5-T Siemens Magnetom Avanto (Siemens Healthcare)

suite. The applicators were placed into the tumour under guidance of MR fluoroscopic sequences. A steady-state free precession sequence which allowed different image weightings to be acquired was used for targeting (BEAT_IRTT sequence, Siemens Corporate Research, Princeton, New Jersey, USA; Fig. 2). A T2-like image weighting was selected if the lesion to be treated was T2 hyperintense or if the visualisation of vessels was considered helpful for orientation or patient safety. T1-weighted images were chosen for targeting T1 hypointense lesions or if previously treated tumour areas required visualising. They were also selected for a number of T1 hyperintense melanoma metastases. Three image planes were selected: two in the plane of the planned applicator track and a third positioned orthogonally to the others. The three images were displayed parallel on the same screen; the update rate of a single slice was 330 ms. Sequence details are given in Table 1. Targeting was performed in one or two steps with intermittent pauses for image monitoring, if necessary. In no case did the procedure have to be aborted as a result of inability to target the lesion. The T1-weighted images acquired during these pauses were used to readjust the slice orientation or needle position. Singular RF applicators were positioned centrally into the target lesion; if two or more applicators were used, these were positioned circumferentially. Energy application was adapted according to the guidelines of the manufacturer, pain level and the size of the active tip. During energy application, the increase of impedance, indicated by a decrease in current level T1-weighted images were acquired to visualise the developing ablation zone and to check for remaining tumour tissue. Energy application was continued if remaining vital tumour tissue was suspected or if the expansion of the T1 hyperintense ablation zone did not include a safety margin of at least 5 mm of healthy liver tissue (Fig. 3). The applicators were repositioned to enclose the entire tumour within the ablation zone if a further expansion of the zone could not be achieved otherwise. Applicator retraction was performed under coagulation. The duration of energy application and, if available, the applied energy were registered.

T1-, T2- and diffusion-weighted images were acquired before definitive applicator retraction in order to exclude remaining T1 hypointense or T2 hyperintense areas with restricted diffusivity, depending on the initial tumour signal behaviour. For diffusion-weighted imaging, the applicator was retracted 3–4 cm in order to decrease probe artefacts. In a number of cases temperature-sensitive measurements were performed by applying the proton resonance frequency shift (PRF) method [21]. A breath-hold gated echo-planar imaging sequence was used to generate phase images in different slice angulations before and directly after energy application. The

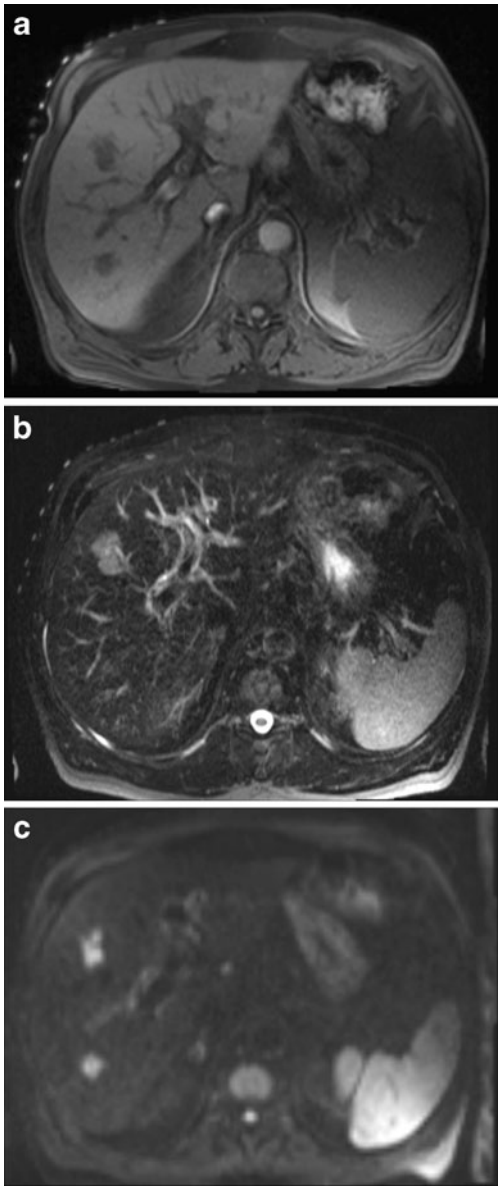

Fig. 1 Pre-interventional T1- **a**, T2- **b** and diffusion-weighted **c** images of a 66-year-old male patient with four metachronous metastases of colorectal cancer, here in liver segment V with a diameter of 29 mm and in liver segment VI with a diameter of 12 mm. An orientation grid and a hyperintense capsule were used to plan the puncture site. The lesions are T1 hypointense, T2 hyperintense (only the lesion in segment V can be seen) and show decreased diffusion

occurring phase changes correlate with the temperature changes and were used to calculate voxel-specific temperature maps [22].

A post-interventional control examination was performed to evaluate the technical success and to exclude complications such as haematomas, active bleeding or perfusion deficits. T1- and T2-weighted transverse slices were acquired, followed by a T1-weighted, contrast-enhanced dynamic liver examination using a volumetric interpolated breath-hold examination (VIBE) sequence [23] after intravenously injecting 0.1 mmol of gadobutrol per kg body weight [24] (Gadovist 1.0, Bayer HealthCare, Leverkusen, Germany). Three measurements were performed within the first 60 s following the automatic injection of contrast agent. The patients were discharged the following day if blood count, abdominal ultrasound and chest radiograph were satisfactory.

Follow-up imaging

All patients received clinical aftercare and a follow-up imaging scheme using MR liver examinations. The first examination was performed 4 weeks after the intervention, and then every 3 months during the first year and every 6 months for next 3 years. After 4 years, one MR liver examination was performed every year. If the follow-up examinations differed from this scheme, the actual intervals in months were calculated. A 1.5-T MR system was used for all examinations (Siemens Magnetom Avanto). T2-weighted HASTE and turbo spin echo sequences using the navigator technique and T1-weighted turbo spin echo sequences using the breath-hold technique were performed. Echo planar imaging sequences were used for diffusion-weighted images using *b* values of 0, 400 and 800 s/mm^2 [25]. A contrast-enhanced dynamic liver examination using VIBE sequences was performed following the intravenous injection of 0.1 mmol of gadobutrol per kg body weight.

Data analysis

Technical success was assessed on the basis of the control examination performed directly post-interventional in the wide-bore 1.5-T system. Depending on the initial signal behaviour of the lesion, the intervention was classified as technically successful if no remaining tumour tissue was detected. The late phase of the contrast-enhanced dynamic liver study was used as a gold standard for evaluating the ablation zone [26]. The ablation zone should be non-enhancing and without nodular contrast enhancement at its edges, which would be signs of remaining tumour tissue. The presence (or absence) of a minimal safety margin of at least 5 mm in all directions was stated in the clinical report. A lack of safety margin was not classified as a technical failure. The same criteria were used for evaluating local tumour progression in the follow-up imaging. Residual tumour was defined as evidence of tumour tissue adjacent to the ablation zone in the control examination 1 month after therapy. Technique effectiveness was defined as complete ablation 1 month after therapy (Fig. 4). Local tumour progression was defined as evidence of vital tumour tissue adjacent to the ablation zone in the subsequent examinations [27].

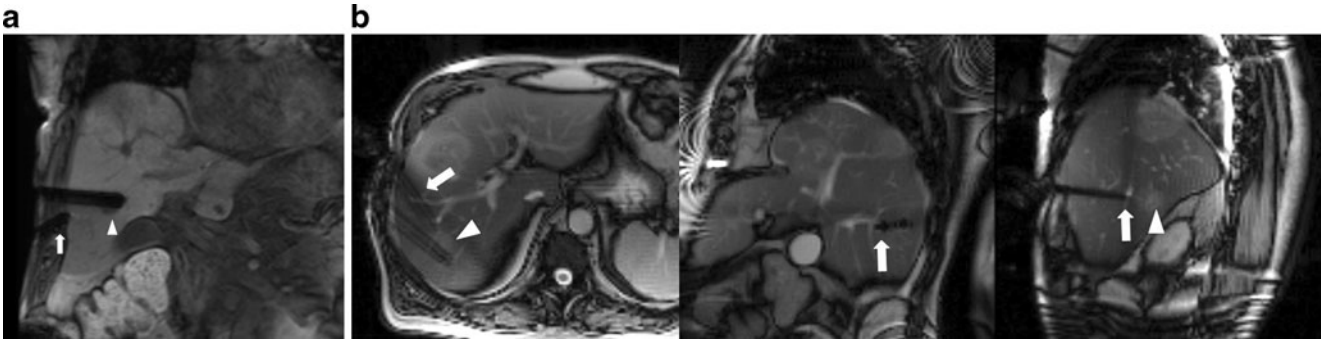

Fig. 2 **a** Coronal slice of a predominantly T1-weighted steady-state free precession sequence of the same patient. A second applicator (*arrow*) is directed to the same tumour and will be placed caudal to the first applicator. A part of the tumour can be seen caudal to the tip of the first applicator (*arrowhead*). **b** A predominantly T2-weighted steady-state free precession sequence with parallel display of a transversal, a sagittal oblique and a coronal oblique image slice used for targeting a second applicator (*arrow*) close to a branch of the portal vein which has to be crossed to reach the target region (*arrowhead*)

Statistical analysis

Fisher's test was used to evaluate whether the differences in local tumour progression between hepatocellular carcinomas (n=43) and all other lesions treated (n=170) were significant. A linear correlation was calculated to analyse the relationship between lesion diameter and duration of energy application.

Results

Technical success

Of 213 treated lesions, 209 were completely ablated, corresponding to a technical success rate of 98.1 %. In 3 cases, treatment had to be stopped before the ablation zone was

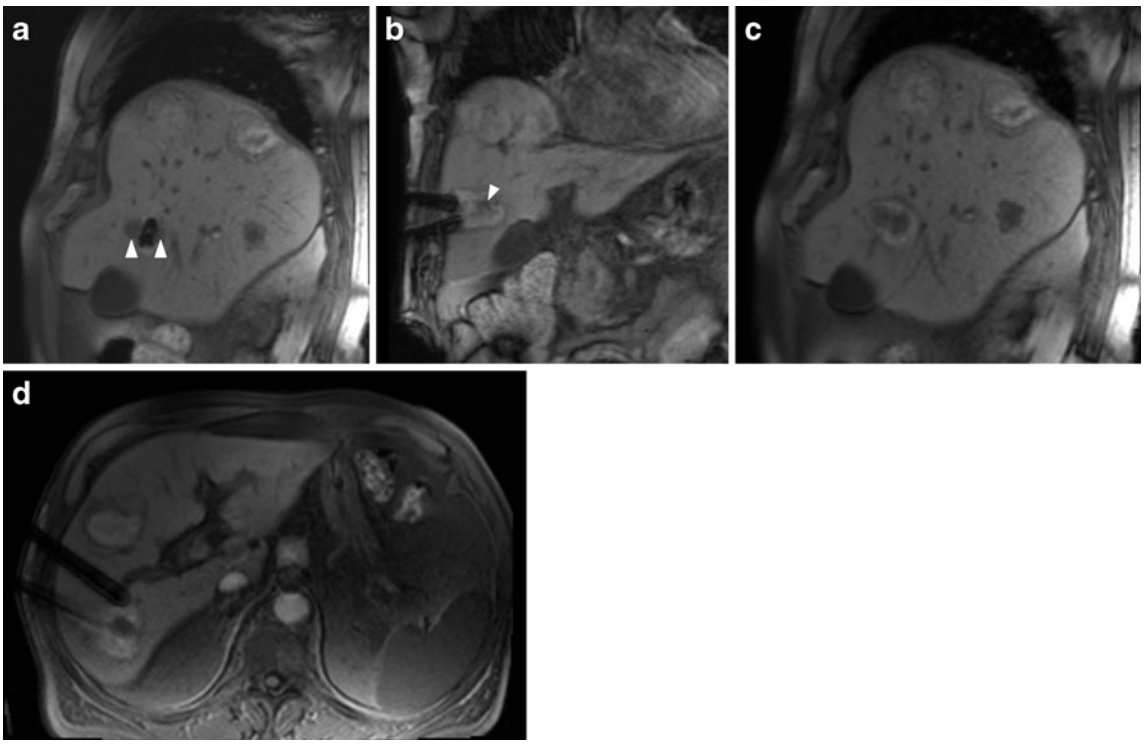

Fig. 3 **a** After energy application to the lesion in segment V, a T1 hyperintense region can be seen around the two hypointense tips of the applicators which were crossed orthogonally during that slice. T1 hypointense tissue is still visible ventral and dorsal to the applicators corresponding to viable tumour (*arrowheads*). Two ablation zones from previous RF therapies are located in liver segment VIII and VII; a viable lesion can be seen in segment VI. **b** On a coronal image, the initial tumour (*arrowhead*) can be differentiated as a hypointense area within the hyperintense ablation zone after retracting the applicators. As it is surrounded by a T1 hyperintense rim, it can be interpreted as a treated, non-viable lesion. **c** After repositioning the probes and further ablation, the ventral and dorsal portions of the tumour are also ablated. **d** Transversal image before definitive retraction of the applicators shows a sufficient safety margin around the tumour

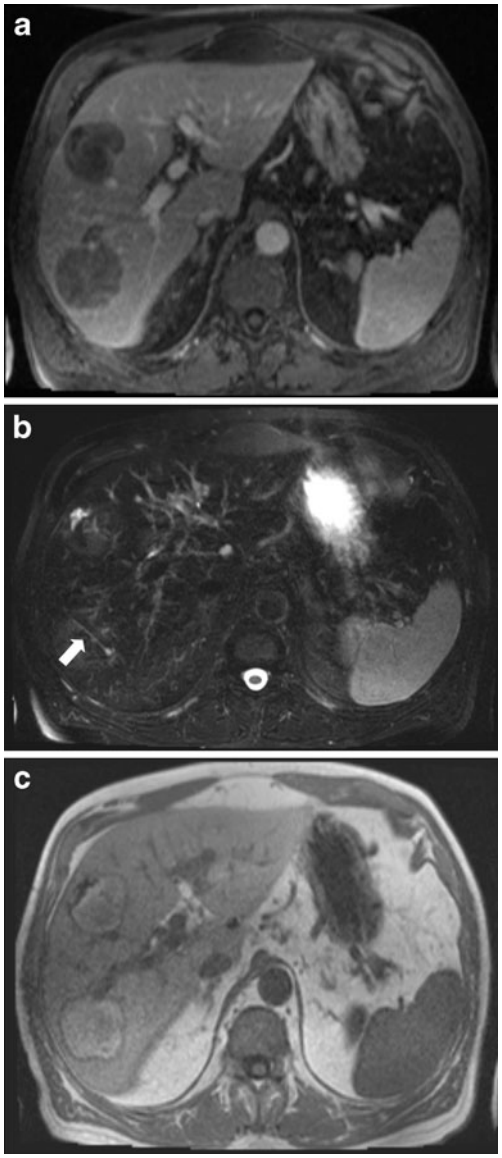

Fig. 4 One month after therapy, the two coagulation zones were not enhancing in the contrast-enhanced dynamic liver examination and presented as T2 hypointense and T1 hyperintense zones. Note the T2 hyperintense previous needle track which filled with blood products and inflammatory cells (*arrow*)

complete because of restrictions in treatment time or pain management. In a fourth case, remaining tumour was detected in the post-interventional control imaging. In 1 case of unsuccessful treatment, therapy was completed during a second intervention 10 days after the first treatment. One other patient underwent surgical resection and 2 patients had rapidly progressive disease without further interventional options.

The lesions were treated using 2.4±1.3 applicator positions; 1–10 applicator positions were necessary for a single lesion. The mean number of applicators used was 1.8 (range 1–4). Mean total duration of energy application was 52± 10 min; the shortest ablation duration was 10 min, the longest 146 min. Mean application duration was 29± 13 min with the cluster probes (tumour size 20±9 mm), 37±27 min using the single monopolar system (tumour size 14±7 mm), 56±28 min using the multipolar approach (tumour size 20±10 mm) and 62±30 min with the single bipolar applicator (tumour size 10±4 mm). Mean energy applied was only available using the bi- and multipolar RF system: it was 102.4±61 kJ with a range between 15 and 255 kJ. Mean initial power output was 44 W for the bipolar system, 138 W using the monopolar cluster system and 55 W for the monopolar single electrode. Mean long axis diameter of the ablation zone was 40.9±11.2 mm (range 17–93 mm), and the mean short axis diameter was 30.2±8.8 mm (range 12–70 mm). The duration of the entire intervention including planning and control examination was between 2 and 6 h (mean 3.7 h); during this time an average of 1.4 (range 1–3) lesions were treated. Duration of energy application only weakly correlated with lesion size (r^2=0.39) and the number of applicator positions (r^2=0.23). There was no correlation between the number of applicator positions and the long axis diameter of the ablation zone (r^2=0.09).

In a small number of cases, diffusion-weighted imaging showed areas of restricted diffusivity which were interpreted as viable tumour; in these cases, ablation was continued until the restriction of diffusion was no longer detectable. All treated lesions showed at least to some extent T1 hyperintense signal behaviour after treatment. On the basis of a gross visual assessment, the shape and size of the T1 hyperintense areas considered as treated tissue corresponded well to the non-enhancing ablation zones in the post-procedural dynamic examination.

Technique effectiveness and local tumour progression

Technique effectiveness was assessed using a dynamic liver examination 1 month after the intervention. A flow chart illustrates the patients' treatment (Fig. 5). Complete tumour ablation was achieved in 210/213 (98.6 %) lesions. In three patients, treatment could not be completed (see "Technical success").

The mean follow-up period was 24.2 months (range 6–44 months). During the follow-up, 18 cases of local tumour progression were observed (18/210), which corresponds to a local tumour progression rate of 8.6 % and to a technical efficacy of 91.4 % (Table 2, Fig. 6). Among these 18 local tumour progressions, 13 lesions were colorectal cancer liver metastasis, 2 lesions were metastases of cholangiocellular carcinoma, 1 lesion was a metastasis of breast cancer and another lesion was from bronchial carcinoma. One case of local tumour progression was observed after RF ablation of a hepatocellular carcinoma. Local tumour progression rate was 17/170 (10.0 %) for all metastases treated, 13/114 (11.4 %) for colorectal liver metastases and 1/43 (2.3 %) for hepatocellular carcinomas. The difference between colorectal liver metastases

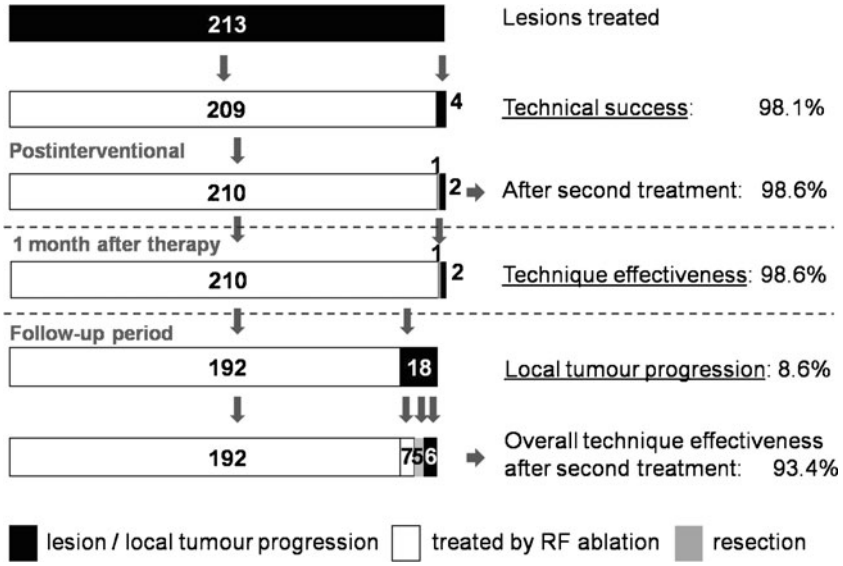

Fig. 5 Flow chart of the 213 lesions treated. *Bars* indicate the characteristics of the lesions in a chronological sequence from the *top* down. *Black bars* represent viable tumour

and hepatocellular carcinomas was not significant (P=0.08) with regard to the local progression rate. Mean duration between RF ablation and detection of local tumour progression was 11.7±6.4 months. The earliest detection of local tumour progression was 4 months after therapy, and the latest was 28 months. The mean initial size of the lesions with local tumour progression was 20.6±8.4 mm. The mean largest ablation zone diameter in these lesions was 44.2±11.7 mm and the mean smallest diameter of the ablation zone was 32.9± 7.2 mm. In three of the lesions, the safety margin had initially been classified as insufficient. All local tumour progressions appeared at the outer edge of the ablation zone.

Seven of the 18 lesions with local tumour progression were successfully retreated using RF ablation, leading to an overall technique effectiveness of 199/213 (93.9 %). Another five local progressive lesions and one incompletely ablated lesion were surgically resected, leading to an overall local therapy effectiveness of 205/213 (96.2 %).

New intrahepatic lesions occurred in 28/110 patients (25 %), and a total of 41/110 (37 %) patients presented new intra- or extrahepatic tumour manifestations during the follow-up period. Seventeen of the patients with new intrahepatic lesions were treated with a second interventional treatment 4–32 months after the first RF ablation. Eight patients died during the follow-up period. Three patients underwent liver transplantation and three other patients underwent hemihepatectomy due to new intrahepatic manifestations which could not be treated interventionally.

Complications and side effects

No major complications occurred on the day of intervention [27]. Following 157 interventions, two major periprocedural complications occurred; the major complication rate was 1.3 %. Bleeding occurred 1 day after the intervention in a 55-year-old male patient with a 35-mm subcapsular HCC lesion in liver segment VIII. Haemoglobin count decreased from 13.1 to 10.2 g/dL during the first post-interventional day. CT showed a perihepatic haematoma but no active bleeding and the patient stabilized without further interaction. Another major complication occurred in a 76-year-old patient with a metastasis from cholangiocelluar carcinoma in liver segment IVa with a diameter of 18 mm. The patient had received RF ablation in liver segment IVb and a segmental cholestasis and presented 1 week after the intervention with fever and gastric pain. Ultrasound and MR dynamic liver examination revealed an infected biloma measuring 45 mm which was interventionally drained and treated with intravenous antibiotics. This patient required a 2-week hospitalisation. Both patients recovered completely. Heat-induced injury of other organs was not observed.

Minor complications occurred in a number of patients. A subcapsular haematoma occurred subsequent to puncture in 8/157 patients, and did not require further action. Three patients with liver cirrhosis presented with post-interventional ascites 1 day after the intervention without accompanying decreases of blood count levels. One patient presented with a small pleural effluence after the intervention, and recovered completely after 1 month. One patient developed a segmental cholestasis in liver segment IV which was diagnosed in the first control examination, and another patient developed segmental cholestasis of the left liver lobe 4 months after the intervention. The minor complication rate was 14/157 (8.9 %).

Discussion

Patient safety and therapy outcome depend, among other factors, on the image investigation used to monitor therapy. Magnetic resonance imaging was proposed for RF ablation

Table 2 Patients presenting with local tumour progression

Patient number	Sex	Age (years)	Lesion type	Location (liver segment)	Lesion size (mm)	RF system	Number of applicator positions	Total energy applied (kJ)	Application duration (min)	Local tumour progression after (months)	Treated
8	m	72	HCC	III	14	Mono-S	3	n/a	43	10	RFA
11	m	60	CRLM	VI	9	Mono-S	3	n/a	38	16	Resection
11	m	60	CRLM	VIII	10	Mono-S	3	n/a	36	7	Resection
15	m	73	CRLM	II	20	Mono-C	2	n/a	24	7	RFA
19	m	80	CRLM	VI	14	Bipolar	1	70	68	10	RFA
19	m	80	CRLM	VI	24	Multi-2	6	240	67	13	Systemic
22	m	92	CRLM	IVa	31	Multi-2	2	60	30	10	Systemic
23	m	69	Lung	VIII	30	Multi-2	4	95	53	4	Systemic
26	m	68	CRLM	IVb	29	Multi-2	8	137	120	10	Systemic
26	m	68	CRLM	IVb	16	Multi-2	2	70	60	22	Systemic
38	m	80	CRLM	II	35	Multi-2	7	185	98	7	RFA
40	m	54	CRLM	VI	19	Multi-2	2	110	45	7	Resection
45	w	64	CRLM	VIII	21	Multi-2	6	170	60	16	Resection
47	w	42	CRLM	VI	9	Multi-2	4	80	30	22	Resection
48	m	68	CRLM	VI	18	Multi-2	6	195	68	28	RFA
55	w	64	CCC	III	13	Multi-2	4	70	35	7	RFA
85	w	55	Br-Ca	VIII	36	Multi-2	8	260	105	7	RFA
105	m	72	CCC	IVb	22	Multi-2	6	120	53	7	Systemic

In the case of systemic tumour manifestations, no local tumour ablation or resection was performed

HCC hepatocellular carcinoma, *CRLM* colorectal liver metastasis, *lung* bronchial carcinoma, *Br-CA* breast cancer, *CCC* cholangiocellular carcinoma, *mono-S* monopolar single applicator, *mono-C* monopolar cluster applicator, *bipolar* single bipolar applicator, *multi-2* two bipolar applicators, *n/a* not applicable, *systemic* patient was treated by chemotherapy

for several reasons. Small tumours can be reliably visualised, the applicators can be positioned under image guidance even at difficult locations and, most importantly, treated tumours can be differentiated from remaining viable tumour. Initially, low-field-strength MR systems were proposed for RF ablation [18, 28–30]. The use of 1.5-T systems allows for increased signal-to-noise ratio, faster image acquisition and the availability of all slice orientations for therapy monitoring when implementing the breath-hold technique [31, 32]. This is an advantage over 0.2-T systems, where dynamic liver examinations and T1-weighted coronal images of the abdomen are difficult to obtain. However, image-guided applicator placement has only really become possible since 1.5-T systems with a wide bore have become available [33]. To our knowledge, this is the largest patient series treated using 1.5 T with MR-guided RF ablation including follow-up that has been published up to now.

The planning examination began using a coronal half acquisition single shot turbo spin echo (HASTE) sequence which allowed for an anatomic overview and a rapid planning of the following sequences within a short period of time. As healthy liver parenchyma often contains more fat than the liver lesions, the T1W in- and out-of-phase imaging could be used in these cases to better define the borders of the lesions.

In the majority of the lesions, various applicator positions were necessary and the completeness of overlapping ablation zones had to be monitored. Whereas with low-field-strength MR systems the T2W images were considered decisive for evaluating the ablation zone [34], the therapy decision in our study was based on T1W images, where treated areas show T1 hyperintense signal behaviour [26]. One advantage of MR therapy monitoring is the possibility of repeatedly visualizing the therapy effects without using a contrast agent [19]. T1W images clearly depict the applicator position within the developing ablation zone [35]. Additional sequences were acquired during therapy, such as T2- or diffusion-weighted imaging. In some cases these provided additional information and influenced the therapeutic decisions. As they were not applied systematically, the value of temperature-sensitive measurements cannot be defined in this study. A small group of patients (partially included here) was systematically analysed elsewhere [22]. Temperature measurements could improve patients' safety by protecting sensitive structures close to the target tissue from heat injury. Furthermore, they have the potential to predict the developing ablation zone which could contribute to the role of MR in therapy monitoring [22].

The relatively high technical success rate reflects the high standard of therapy monitoring at 1.5 T and justifies the use of T1-weighted images to characterize the ablation zone. However, a systematic comparison of the T1 hyperintense areas with the non-enhancing ablation zones in the post-procedural control scans was not performed. The T1 hyperintense changes within the ablation zone may not necessarily span the entire area of tissue necrosis; additionally, the

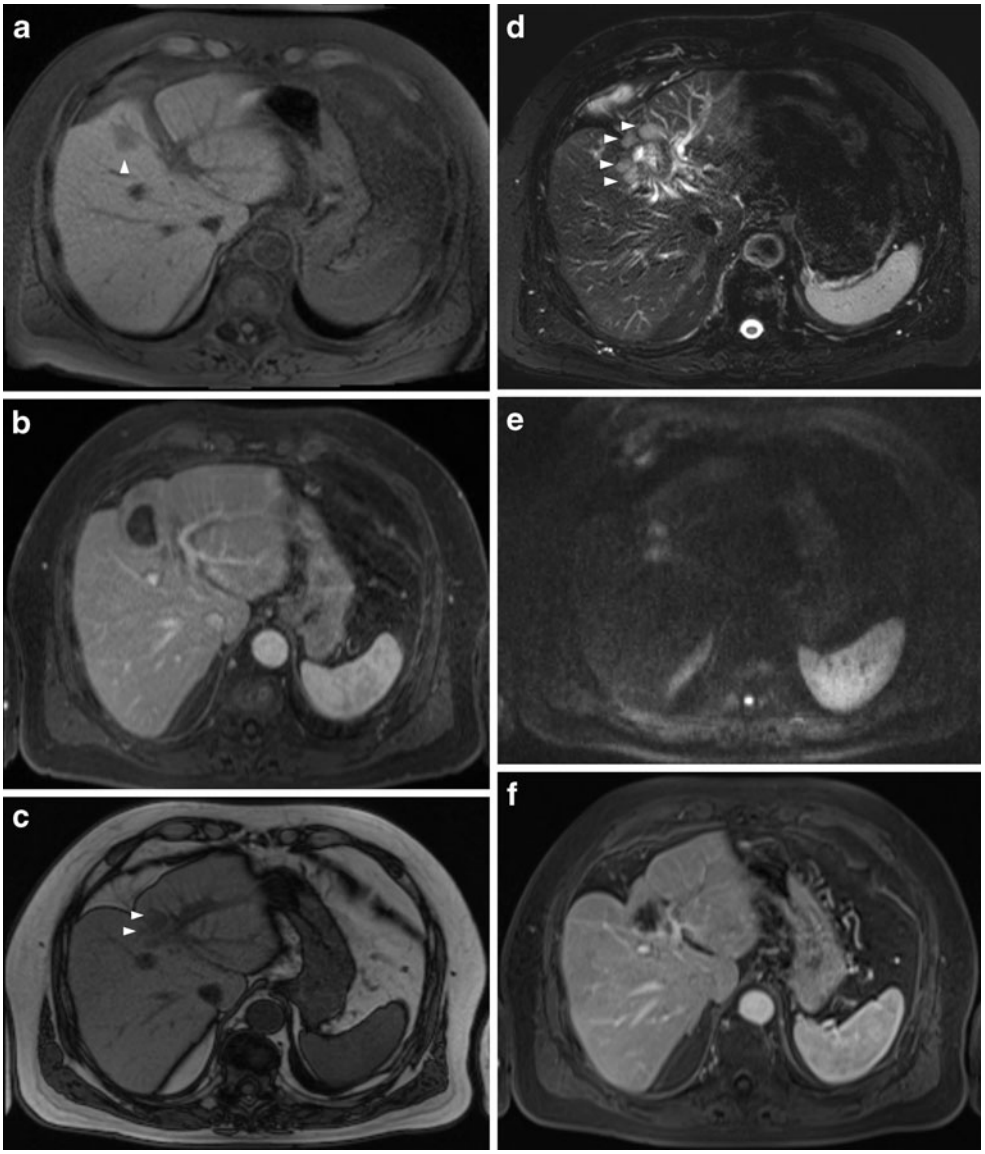

Fig. 6 **a** 69-year-old male patient presenting with a singular metastasis of a resected extrahepatic cholangiocellular carcinoma in segment IV with a diameter of 22 mm. **b** One month after RF ablation, the non-enhancing zone was classified as completely ablated. **c** Seven months after therapy, a multifocal local tumour progression was detected in the T1- and T2-weighted **d** sequences and the diffusion-weighted imaging **e**, whereas it was more difficult to detect the local tumour progression in the dynamic liver examination **f**

change of the T1 signal during ablation may be delayed, and both effects could lead to an underestimation of the actual ablation zone.

Applicator positioning requires precise visualisation of the target lesion and the applicator, ideally in different slice positions and with a fast image update rate. The sequence used for targeting fulfilled all of these requirements and had additional advantages compared to CT, where fluoroscopic needle placement is not possible without radiation exposure. During the selection of slice thickness for the BEAT_IRTT sequence, a compromise had to be found between signal outcome and visualisation of small lesions. For the BEAT_IRTT sequence, a slice thickness of 12 mm provided a sufficient image quality; however, the visualization of small lesions was decreased due to the partial volume effect. This is especially a problem in case of very small HCC lesions without T2 signal hyperintensity. Anatomic landmarks such as vessel bifurcations may be used to increase orientation during fluoroscopic imaging. The use of a liver-specific contrast agent might help to identify such targets [36, 37]. MR-guided RF ablation is comparably time-intensive. A number of expandable RF applicators are not MR-compatible and multiprobe approaches with various applicator positions need additional time for targeting. The long therapy duration is cost-intensive, as several patients could be examined during the time needed for one such intervention. CT- and ultrasound-guided interventions are less time-intensive and technically less complex, resulting in considerably lower costs. An alternative to MR-guided ablation allowing for immediate ablation control is contrast-enhanced ultrasound, which is less expensive, available and does not require special material [38, 39]. However, visibility may be reduced depending on the patient and the location of the target lesion in the liver and (repeated) intravenous application of a safe contrast agent is necessary.

MR-guided ablation will be reserved mainly for medical centres. Its major strength lies in the ability to monitor the treatment effect during the procedure. It may be especially helpful for larger lesions requiring several overlapping ablation zones and tumours in difficult localizations. A high technical success rate improves the prognosis of the patients [40] which may increase the acceptance by patients and clinical partners; and a low rate of tumour progression decreases the overall costs for the health care system.

However, despite the high technical success rate, the rate of local tumour progression in our series still seems too high. Comparison with other patient series treated under MR guidance is difficult due to smaller cohort sizes and shorter follow-up periods; complete tumour ablation ranged between 51 and 93 % in mixed patient groups of between 4 and 64 patients and follow-up periods between 2 and 24 months [28, 30, 31, 41, 42]. A definitive evaluation of the therapy approach will only be possible based on 5-year survival rates and larger, homogeneous patient cohorts. Studies using ultrasound and CT for RF ablations reported primary technical success rates of 83–93 % for hepatocellular carcinomas [1, 43, 44] and 97–98 % for liver metastases [4, 45]. Major complication rates range between 0 and 5 % using CT-guided RF ablation [43, 45] and between 1 and 4 % using ultrasound [1, 4, 44, 46]. However, some studies using ultrasound report that up to 3.3 sessions were required to completely treat the lesions [1, 44]. Local tumour recurrence rates of ultrasound-guided RF ablation ranged between 10 and 24 % for hepatocellular carcinomas; one study using CT reports a local recurrence rate of 22 % during a mean follow-up of 29 months [1, 44, 47, 48]. Local tumour recurrence rates after percutaneous RF ablation of liver metastases were reported to be 39 % and 42.5 % using ultrasound or a combination of ultrasound and CT (mean follow-up 25 and 38 months), respectively [4, 45]. Although tumour sizes, treatment protocols and follow-up imaging vary between the cited series, it may be concluded that MR-guided RF ablation may have the potential to achieve lower local recurrence rates for both hepatocellular carcinomas and liver metastases.

All tumour progressions observed in our patients occurred at the edge of the ablation zone and must be interpreted as indicative of insufficient safety margins. Previous studies have reported on the importance of safety margins, as well as the relationship between initial tumour size and local tumour progress rate [8, 49]. Although the mean safety margins based on the measured tumour diameters and ablation zones seemed adequate, focal insufficient margins were detected in various cases and may be responsible for the local progressions.

This study was not designed to evaluate the different RF systems used. Mean lesion diameters differ between the RF systems as well as the number of applicators implemented in the multipolar approach, so that a systematic analysis is not possible. Independent from tumour diameter, the duration of energy application was shortest with the monopolar cluster applicator and longest for the single bipolar applicators. Local tumour progression was observed for all RF systems except the multipolar approach with three or four applicators used in 18 cases.

The validity of our analysis is limited due to the mixed and restricted follow-up duration and the heterogeneous pathology of the tumours. This therapeutic approach should be evaluated with homogeneous patient groups and based on the 5-year-survival rate. A blinded control of the T1-based therapy monitoring was not performed.

In conclusion, MR-guided RF ablation is a safe and efficient therapy option for liver tumours. MR guidance facilitates applicator placement and therapy monitoring allowing the differentiation of viable tumour from treated parenchyma. A decrease of the T1 relaxation time can be used to reliably predict the developing ablation zone. Careful attention should be given to creating a sufficient safety margin to avoid local tumour progression.

Acknowledgement Thanks to Li Pan from Siemens Research for the development and provision of real-time MR sequences for applicator placement.

References

1. Lencioni R, Cioni D, Crocetti L et al (2005) Early-stage hepatocellular carcinoma in patients with cirrhosis: long-term results of percutaneous image-guided radiofrequency ablation. Radiology 234:961–967
2. Gillams AR, Lees WR (2009) Five-year survival in 309 patients with colorectal liver metastases treated with radiofrequency ablation. Eur Radiol 19:1206–1213
3. Goldberg SN, Ahmed M (2002) Minimally invasive image-guided therapies for hepatocellular carcinoma. J Clin Gastroenterol 35: S115–S129
4. Solbiati L, Livraghi T, Goldberg SN et al (2001) Percutaneous radio-frequency ablation of hepatic metastases from colorectal cancer: long-term results in 117 patients. Radiology 221:159–166
5. Bonastre J, De Baere T, Elias D et al (2007) Cost of radiofrequency ablation in the treatment of hepatic malignancies. Gastroenterol Clin Biol 31:828–835
6. Llovet JM (2005) Updated treatment approach to hepatocellular carcinoma. J Gastroenterol 40:225–235
7. Bruix J, Sherman M (2005) Management of hepatocellular carcinoma. Hepatology 42:1208–1236
8. Kudo M (2010) Radiofrequency ablation for hepatocellular carcinoma: updated review in 2010. Oncology 78(Suppl 1):113–124
9. Lee WS, Yun SH, Chun HK et al (2008) Clinical outcomes of hepatic resection and radiofrequency ablation in patients with solitary colorectal liver metastasis. J Clin Gastroenterol 42:945–949
10. Aloia TA, Vauthey JN, Loyer EM et al (2006) Solitary colorectal liver metastasis: resection determines outcome. Arch Surg 141:460–466, discussion 466–467
11. de Baere T, Elias D, Dromain C et al (2000) Radiofrequency ablation of 100 hepatic metastases with a mean follow-up of more than 1 year. AJR Am J Roentgenol 175:1619–1625
12. Mulier S, Ni Y, Jamart J, Michel L, Marchal G, Ruers T (2008) Radiofrequency ablation versus resection for resectable colorectal

liver metastases: time for a randomized trial? Ann Surg Oncol 15:144–157
13. Lin SM, Lin CJ, Lin CC, Hsu CW, Chen YC (2005) Randomised controlled trial comparing percutaneous radiofrequency thermal ablation, percutaneous ethanol injection, and percutaneous acetic acid injection to treat hepatocellular carcinoma of 3 cm or less. Gut 54:1151–1156
14. Machi J, Bueno RS, Wong LL (2005) Long-term follow-up outcome of patients undergoing radiofrequency ablation for unresectable hepatocellular carcinoma. World J Surg 29:1364–1373
15. Mulier S, Ni Y, Jamart J, Ruers T, Marchal G, Michel L (2005) Local recurrence after hepatic radiofrequency coagulation: multivariate meta-analysis and review of contributing factors. Ann Surg 242:158–171
16. Leyendecker JR, Dodd GD 3rd, Halff GA et al (2002) Sonographically observed echogenic response during intraoperative radiofrequency ablation of cirrhotic livers: pathologic correlation. AJR Am J Roentgenol 178:1147–1151
17. Pacella CM, Bizzarri G, Anelli V et al (1998) Evaluation of the vascular pattern of hepatocellular carcinoma with dynamic computed tomography and its use in identifying optimal temporal windows for helical computed tomography. Eur Radiol 8:30–35
18. Lewin JS, Connell CF, Duerk JL et al (1998) Interactive MRI-guided radiofrequency interstitial thermal ablation of abdominal tumors: clinical trial for evaluation of safety and feasibility. J Magn Reson Imaging 8:40–47
19. McDannold N, Jolesz F (2000) Magnetic resonance image-guided thermal ablations. Top Magn Reson Imaging 11:191–202
20. Clasen S, Pereira PL (2008) Magnetic resonance guidance for radiofrequency ablation of liver tumors. J Magn Reson Imaging 27:421–433
21. Hindmann JC (1966) Proton resonance shift of water in the gas and liquid state. J Chem Phys 44:4582–4592
22. Rempp H, Hoffmann R, Roland J et al (2011) Threshold-based prediction of the coagulation zone in sequential temperature mapping in MR-guided radiofrequency ablation of liver tumours. Eur Radiol. doi:10.1007/s00330-011-2335-8
23. Rofsky NM, Lee VS, Laub G et al (1999) Abdominal MR imaging with a volumetric interpolated breath-hold examination. Radiology 212:876–884
24. Lee VS, Lavelle MT, Rofsky NM et al (2000) Hepatic MR imaging with a dynamic contrast-enhanced isotropic volumetric interpolated breath-hold examination: feasibility, reproducibility, and technical quality. Radiology 215:365–372
25. Schraml C, Schwenzer NF, Clasen S et al (2009) Navigator respiratory-triggered diffusion-weighted imaging in the follow-up after hepatic radiofrequency ablation-initial results. J Magn Reson Imaging 29:1308–1316
26. Kierans AS, Elazzazi M, Braga L et al (2010) Thermoablative treatments for malignant liver lesions: 10-year experience of MRI appearances of treatment response. AJR Am J Roentgenol 194:523–529
27. Goldberg SN, Grassi CJ, Cardella JF et al (2009) Image-guided tumor ablation: standardization of terminology and reporting criteria. J Vasc Interv Radiol 20:S377–S390
28. Kelekis AD, Terraz S, Roggan A et al (2003) Percutaneous treatment of liver tumors with an adapted probe for cooled-tip, impedance-controlled radio-frequency ablation under open-magnet MR guidance: initial results. Eur Radiol 13:1100–1105
29. Huppert PE, Trubenbach J, Schick F, Pereira P, Konig C, Claussen CD (2000) MRI-guided percutaneous radiofrequency ablation of hepatic neoplasms—first technical and clinical experiences. Rofo 172:692–700
30. Kettenbach J, Köstler W, Rücklinger E et al (2003) Percutaneous saline-enhanced radiofrequency ablation of unresectable hepatic tumors: initial experience in 26 patients. AJR Am J Roentgenol 180:1537–1545
31. Mahnken AH, Buecker A, Spuentrup E et al (2004) MR-guided radiofrequency ablation of hepatic malignancies at 1.5T: initial results. J Magn Reson Imaging 19:342–348
32. Gaffke G, Gebauer B, Knollmann FD (2006) Use of semiflexible applicators for radiofrequency ablation of liver tumors. Cardiovasc Intervent Radiol 29:270–275
33. Boss A, Rempp H, Martirosian P et al (2008) Wide-bore 1.5 Tesla MR imagers for guidance and monitoring of radiofrequency ablation of renal cell carcinoma: initial experience on feasibility. Eur Radiol 18:1449–1455
34. Chen MH, Wei Y, Yan K et al (2006) Treatment strategy to optimize radiofrequency ablation for liver malignancies. J Vasc Interv Radiol 17:671–683
35. Aube C, Schmidt D, Brieger J et al (2004) Magnetic resonance imaging characteristics of six radiofrequency electrodes in a phantom study. J Vasc Interv Radiol 15:385–392
36. Bathe OF, Mahallati H (2007) MR-guided ablation of hepatocellular carcinoma aided by gadoxetic acid. J Surg Oncol 95:670–673
37. Fischbach F, Bunke J, Thormann M et al (2011) MR-guided freehand biopsy of liver lesions with fast continuous imaging using a 1.0-T open MRI scanner: experience in 50 patients. Cardiovasc Intervent Radiol 34:188–192
38. Solbiati L, Ierace T, Tonolini M, Cova L (2004) Guidance and monitoring of radiofrequency liver tumor ablation with contrast-enhanced ultrasound. Eur J Radiol 51(Suppl):S19–S23
39. Wiggermann P, Zuber-Jerger I, Zausig Y et al (2011) Contrast-enhanced ultrasound improves real-time imaging of ablation region during radiofrequency ablation: Preliminary results. Clin Hemorheol Microcirc 49:43–54
40. Takahashi S, Kudo M, Chung H et al (2007) Initial treatment response is essential to improve survival in patients with hepatocellular carcinoma who underwent curative radiofrequency ablation therapy. Oncology 72(Suppl 1):98–103
41. Clasen S, Rempp H, Boss A et al (2011) MR-guided radiofrequency ablation of hepatocellular carcinoma: long-term effectiveness. J Vasc Interv Radiol 22:762–770
42. Clasen S, Boss A, Schmidt D et al (2007) MR-guided radiofrequency ablation in a 0.2-T open MR system: technical success and technique effectiveness in 100 liver tumors. J Magn Reson Imaging 26:1043–1052
43. Laspas F, Sotiropoulou E, Mylona S et al (2009) Computed tomography-guided radiofrequency ablation of hepatocellular carcinoma: treatment efficacy and complications. J Gastrointestin Liver Dis 18:323–328
44. Buscarini L, Buscarini E, Di Stasi M, Vallisa D, Quaretti P, Rocca A (2001) Percutaneous radiofrequency ablation of small hepatocellular carcinoma: long-term results. Eur Radiol 11:914–921
45. Gillams AR, Lees WR (2008) Five-year survival following radiofrequency ablation of small, solitary, hepatic colorectal metastases. J Vasc Interv Radiol 19:712–717
46. Shiina S, Teratani T, Obi S et al (2005) A randomized controlled trial of radiofrequency ablation with ethanol injection for small hepatocellular carcinoma. Gastroenterology 129:122–130
47. Camma C, Di Marco V, Orlando A et al (2005) Treatment of hepatocellular carcinoma in compensated cirrhosis with radiofrequency thermal ablation (RFTA): a prospective study. J Hepatol 42:535–540
48. Guglielmi A, Ruzzenente A, Battocchia A, Tonon A, Fracastoro G, Cordiano C (2003) Radiofrequency ablation of hepatocellular carcinoma in cirrhotic patients. Hepatogastroenterology 50:480–484
49. Ng KK, Poon RT, Lo CM, Yuen J, Tso WK, Fan ST (2008) Analysis of recurrence pattern and its influence on survival outcome after radiofrequency ablation of hepatocellular carcinoma. J Gastrointest Surg 12:183–191